Many-body localization transition through pairwise correlations

Jaime L. C. da C. Filho, Andreia Saguia, Lea F. Santos, and Marcelo S. Sarandy

Phys. Rev. B **96**, 014204 — Published 21 July 2017

DOI: 10.1103/PhysRevB.96.014204

Many-body localization transition through pairwise correlations

Jaime L. C. da C. Filho,[1,2,*] Andreia Saguia,[1,†] Lea F. Santos,[3,‡] and Marcelo S. Sarandy[1,§]

[1] *Instituto de Física, Universidade Federal Fluminense, Av. Gal. Milton Tavares de Souza s/n, Gragoatá, 24210-346 Niterói, Rio de Janeiro, Brazil*

[2] *Instituto Federal do Pará - Campus Castanhal, BR 316 Km 61, Saudade II, 68740-970, Castanhal, PA, Brazil*

[3] *Department of Physics, Yeshiva University, New York, New York 10016, USA*

We investigate the phenomenon of spatial many-body localization (MBL) through pairwise correlation measures based on one and two-point correlation functions. The system considered is the Heisenberg spin-1/2 chain with exchange interaction J and random onsite disorder of strength h. As a representative pairwise correlation measure obtained from one-point functions, we use global entanglement. Through its finite size scaling analysis, we locate the MBL critical point at $h_c/J = 3.8$. As for measures involving two-point functions, we analyze pairwise geometric classical, quantum, and total correlations. Similarly to what happens for continuous quantum phase transitions, it is the derivatives of these two-point correlation measures that identify the MBL critical point, which is found to be in the range $h_c/J \in [3, 4]$. Our approach relies on very simple measures that do not require access to multipartite entanglement or large portions of the system.

I. INTRODUCTION

Concepts and tools from quantum information theory have found applications in the development of new numerical methods [1] and in fields as diverse as metrology [2], high energy physics [3], and condensed matter physics [4, 5]. In particular, the successful detection of quantum phase transitions via quantum correlation measures, including concurrence [6, 7], entanglement entropy [8], and quantum discord [9, 10], has motivated the use of these quantities in theoretical [11–19] and experimental [20, 21] studies of the transition to many-body localized phases.

The term "many-body localization" (MBL) usually refers to spatial localization of interacting systems in the presence of onsite disorder. In one-dimensional noninteracting quantum systems, the inclusion of uncorrelated [22] or quasiperiodic [23] onsite disorder takes the system into an insulating phase. In interacting systems, the interplay between interaction and disorder can cause the onset of quantum chaos [24, 25], which greatly enhances delocalization. In these chaotic quantum systems with many interacting particles, the eigenstates away from the edges of the spectrum approach random vectors, therefore enabling the emergence of thermalization [26–29]. It is natural to wonder whether such complex systems, capable of exhibiting statistical behavior despite isolation, may still become spatially localized under finite values of disorder strength.

The viability of MBL was discussed already in Refs. [22, 30, 31] and perturbative approaches were employed to show that it indeed occurs at low temperatures [32, 33]. For highly excited states, analytical [34, 35], numerical [11–13, 15–19, 36–66], and experimental [20, 21, 67, 68] studies also point toward a positive answer. The numerical characterization of the transition to the MBL phase have included the analysis of level statistics [11–13, 25, 37, 40, 57] and its dynamical consequences [65], delocalization measures, such as Shannon entropy and participation ratio [11–13, 39, 42, 64], transport properties [61], as well as power-law decays of the survival probability [50] and few-body observables [46, 49].

From the point of view of quantum information theory, studies of MBL have taken several approaches, including the analysis of entanglement spectrum [17] and entanglement dynamics [69, 70]. It has been shown, for instance, that deep in the chaotic phase, multipartite entanglement is large [12], while a shift to pairwise entanglement takes place in the vicinity of the MBL transition [11–15]. In the localized phase, the entanglement between two sites [39] and the quantum mutual information between two traced-out regions [19] fall off exponentially with their distance. As for the search for the critical point, scaling analysis of total multipartite correlations [18] and of the entanglement entropy [48, 53] have been used. The latter has actually become the most popular method to characterize the MBL transition. In the chaotic (thermal) phase, for any bipartition of the chain, the scaling of the entanglement entropy for the many-body eigenstates away from the edges of the spectrum obeys a volume law, while in the MBL phase, it exhibits an area law. In terms of dynamics, for initial states corresponding to computational basis vectors, as the system approaches the MBL phase, the entanglement entropy [16, 38, 41] as well as the Shannon information entropy [64] and the quantum mutual information [19] grow logarithmically in time, which contrasts with the very fast increase and quick saturation in the chaotic regime.

In the present work, instead of manipulating large parts of the quantum system, as in the case of bipartite blocks, or dealing with multipartite measures, we focus on the characterization of the MBL critical point through pairwise correlation measures that involve one or at most two-point correlation functions. Specifically, we consider global entanglement [71, 72] and pairwise geometric correlations beyond entanglement, as defined in [73–75]. These simple pairwise correlation measures are accessible through quantum tomography, with one- and two-point functions readily provided by

*Electronic address: jaime.filho@if.uff.br
†Electronic address: amen@if.uff.br
‡Electronic address: lsantos2@yu.edu
§Electronic address: msarandy@if.uff.br

current experiments [76–78].

Global entanglement is based on one-point functions only. It can be understood as an average pairwise correlation measure, where the pair consists of a single site and all the rest of the system. By collapsing the global entanglement curves for different system sizes onto a single scaling function, we are able to precisely identify the critical point.

Pairwise correlation measures beyond entanglement were first proposed in Refs. [79, 80]. In this scenario, to classify and quantify physical correlations, one separates the states into quantum and classical, rather than entangled and unentangled. Classical states are defined as those left undisturbed by a non-selective local measurement [81, 82], while the opposite holds for quantum states. Not all separable states are classical, some exhibit quantum correlations [79, 80]. The latter are useful tools in the analysis of critical phenomena due to their robustness at finite temperature [83] and their long-range behavior in critical phases [84].

We investigate pairwise classical, quantum, and total correlations at the MBL transition. To evaluate them, we take a geometric approach, via the trace norm in state space [73–75]. The use of geometric correlations is convenient, because they can be analytically derived for various classes of two-qubit states. We show that, similarly to what happens for ordinary continuous quantum phase transitions, it is the first derivative of these two-point correlation measures that detects the critical point.

II. HEISENBERG SPIN-1/2 CHAINS IN A RANDOM MAGNETIC FIELD

We consider a closed isotropic Heisenberg spin-1/2 chain with N sites and random static magnetic fields in the z-direction. The Hamiltonian is given by

$$H = \sum_{k=1}^{N} \left[J \left(S_k^x S_{k+1}^x + S_k^y S_{k+1}^y + S_k^z S_{k+1}^z \right) + h_k S_k^z \right], \tag{1}$$

where $\hbar = 1$ and $S_k^{x,y,z} = \sigma_k^{x,y,z}/2$, with $\sigma_k^{x,y,z}$ denoting the Pauli operators on site k. The Zeeman splittings h_k are random numbers from a uniform distribution in the interval $[-h, h]$ and J is the exchange interaction. Borrowing the language from quantum information theory, we refer to a spin-1/2 as a quantum bit (qubit).

The model conserves total magnetization in the z-direction, $\mathcal{S}^z = \sum_k S_k^z$, that is $[H, \mathcal{S}^z] = 0$. Our studies focus on the largest subspace, $\mathcal{S}^z = 0$, where localization is more demanding. We exactly diagonalize the Hamiltonian matrix of this block. Our analysis is carried out for 10% of the eigenstates that belong to the middle of the energy spectrum, where they tend to be more delocalized. We perform averages over these states and over disorder configurations. For $N = 10, 12, 14$, we average over 10^4 disorder realizations, while for $N = 16$ we use 10^3 configurations.

The Hamiltonian in Eq. (1) has two integrable limits, one when the chain is clean, h/J=0, and the other for $h/J > h_c/J$, where h_c/J is the MBL critical point. Previous works have estimated $h_c/J \sim 3.8$ [18, 48, 53]. Between the two integrable regions, for $0 < h/J < h_c/J$, the system shows level repulsion and level spacing distributions that vary from the Wigner-Dyson shape, typical of chaotic systems, to a nearly Poisson distribution, which is usual in integrable models [11, 25]. For $N = 16$, the best agreement with the Wigner-Dyson distribution, indicating that the system is deep in the chaotic regime, occurs for $h/J \sim 0.5$ [64].

III. GLOBAL ENTANGLEMENT

Global entanglement, G_E, was introduced in Ref. [71] as a multipartite entanglement measure for pure composite states. It vanishes if, and only if, the state is a tensor product of all of its subsystems. As shown in Ref. [72], the measure can be expressed in terms of an average over pairwise entanglement between one site and the rest of the system. More specifically, $G_E(|\psi\rangle)$ is obtained from the one-qubit reduced density operators as

$$G_E(|\psi\rangle) = 2 - \frac{2}{N} \sum_{k=1}^{N} \mathrm{Tr}\left(\rho_k^2\right). \tag{2}$$

If translation invariance is obeyed, Eq. (2) reduces to

$$G_E(|\psi\rangle) = 2\left[1 - \mathrm{Tr}\left(\rho_1^2\right)\right], \tag{3}$$

where $\rho_1 = \rho_k$, $\forall k$. Equation (3) is the linear entropy for a single spin of the system.

Note that G_E does not require direct access to large portions of the system. As provided by Eq. (3), global separability is locally manifested through one-point functions only, with the rest of the system being traced out. General properties of G_E in random localized states of disordered systems were considered in Ref. [85]. The dependence of global entanglement on the disorder strength was studied also in [13], although the characterization of the MBL critical point was not provided.

The analysis of the MBL transition via global entanglement can be done directly with Eq. (3), because the average over disorder realizations implies that all sites are equivalent. Our results are shown in Fig. 1. As h/J increases and the system approaches the MBL phase, the value of global entanglement decreases, since more entanglement gets localized in smaller subsystems, such as in pair of spins.

The crossing of the curves in the main panel of Fig. 1 indicates the approximate value of the critical point, which is then precisely obtained through a finite size scaling analysis. This is done by choosing the scaling form

$$G_E = \Phi\left[N^a \left(\frac{h - h_c}{J}\right)\right], \tag{4}$$

where Φ is a function determined by the chi-square minimization method. This function is employed in the scaling analysis presented in the inset (a) of Fig. 1. We find that $a = 0.5$ and $h_c/J = 3.8 \pm 0.2$. It is impressive that G_E, which corresponds to the linear entropy of a single spin, can determine

the critical point in such excellent agreement with previous studies [18, 48, 53].

In the inset (b) of Fig. 1, we show the behavior of G_E deep in the localized phase in a logarithmic scale. Note that it exhibits a power-law decay, $G_E \propto (h/J)^{-\alpha}$, with exponent roughly given by $\alpha = 1$. This behavior closely resembles the multipartite mutual information, as discussed in Ref. [18].

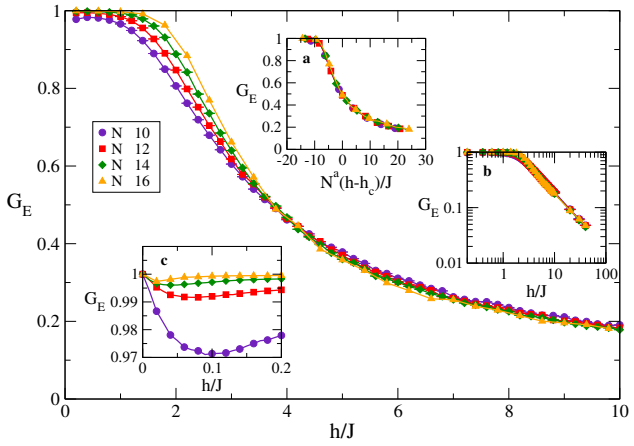

FIG. 1: (Color online) Main panel: Global entanglement G_E as a function of the disorder strength h/J. Inset (a) shows the finite size scaling analysis, with $a = 0.5$ and $h_c/J = 3.8 \pm 0.2$. Inset (b) shows the power-law decay of G_E in the localized phase. Inset (c) shows the non-monotonic behavior of G_E for small values of h/J.

We also notice that G_E presents a non-monotonic behavior for small values of h/J. This is shown in the inset (c) of Fig. 1. The maximal value, $G_E = 1$, occurs in the clean integrable limit, as originally shown in Ref. [71]. As h/J increases from zero, G_E shows a minor dip, before reaching very large values again in the chaotic regime. Analogously to what happens to quantities that measure the integrable-chaos transition [64], the dip shifts towards smaller h/J's as the system size increases. This suggests that, in addition to identifying the MBL critical point, G_E may be a general integrable-chaos detector. Whether this non-monotonic behavior will persist in the thermodynamic limit is a subject that requires further investigation.

IV. GEOMETRIC CORRELATIONS FOR TWO-QUBIT STATES

Pairwise correlations are analyzed in a bipartite Hilbert space $\mathcal{H} = \mathcal{H}_1 \otimes \mathcal{H}_2$. The quantum states of the composite system are described by density operators $\rho \in \mathcal{B}(\mathcal{H})$, where $\mathcal{B}(\mathcal{H})$ is the set of bound, positive-semidefinite operators acting on $\mathcal{H}$ with trace given by $\mathrm{Tr}\,\rho = 1$. To distinguish classical from quantum correlation measures, we use the concept of classicality in quantum information. A state is classical if it is not disturbed under projective measurements [81]. Let us denote a set of local von Neumann measurements as $\{\Pi_1^j \otimes \mathbb{1}_2\}$, where Π_1^j is a set of orthogonal projectors over the first subsystem of the bipartition. After a non-selective measurement M, the density operator ρ becomes

$$M(\rho) = \sum_j [\Pi_1^j \otimes \mathbb{1}_2]\, \rho\, [\Pi_1^j \otimes \mathbb{1}_2]. \tag{5}$$

If there exists any measurement M such that $M(\rho) = \rho$, then ρ describes a hybrid state, referred to as classical-quantum state, which is classical with respect to the Hilbert space $\mathcal{H}_1$ and potentially quantum with respect to $\mathcal{H}_2$. Extension of this definition for measurements over all subsystems and for multipartite states can be found in [82]. We emphasize that separable mixed states are not necessarily classical and may still present quantum correlations. Therefore, non-classical states are not necessarily quantum entangled.

We define pairwise correlation measures by adopting a geometric approach based on the general formalism introduced in Refs. [86–88]. We consider correlations based on the trace norm (Schatten 1-norm) and projective measurements operating over $\mathcal{H}_1$. The three kinds of correlations analyzed here are pairwise geometric classical, quantum, and total.

The amount of quantum correlation is measured through the geometric quantum discord, $Q_G(\rho)$, defined as

$$Q_G(\rho) = \min_{\{M\}} \mathrm{Tr}\,|\rho - M(\rho)|\,. \tag{6}$$

The minimization is taken over all local measurements M acting on $\mathcal{H}_1$. Thus, $Q_G(\rho)$ represents the distance between ρ and the closest classical-quantum state obtained by measuring ρ.

The amount of classical correlation $C_G(\rho)$ associated with ρ is obtained from

$$C_G(\rho) = \max_{\{\bar{M}\}} \mathrm{Tr}\left|\bar{M}(\rho) - \bar{M}(\pi_\rho)\right|, \tag{7}$$

with the maximization done over all local measurements $\bar{M}$ acting on $\mathcal{H}_1$ and $\pi_\rho = \rho_1 \otimes \rho_2 = \mathrm{Tr}_2\rho \otimes \mathrm{Tr}_1\rho$. To avoid ambiguities in the correlation measures for Q_G and C_G, we take M and $\bar{M}$ as independent measurement sets [88]. The classical correlation $C_G(\rho)$ relates to the maximum information about the state that we can locally extract by measuring ρ. It vanishes if and only if ρ is a tensor product of its marginals, that is, if ρ is the completely uncorrelated state π_ρ.

For the total correlation, we simply take the trace distance between ρ and π_ρ, which yields

$$T_G(\rho) = \mathrm{Tr}\,|\rho - \pi_\rho|\,. \tag{8}$$

The total correlation as provided by Eq. (8) detects any kind of correlation that makes ρ distinct from the trivial product state π_ρ.

Here, we study the correlations between two spins only and choose those that are nearest neighbors in the quantum spin chain. To provide some intuition about the correlation measures considered in this work, let us begin by analyzing a two-spin quantum system, with $\{|00\rangle, |01\rangle, |10\rangle, |11\rangle\}$ denoting the computational basis. A quantum state exhibits correlation (either classical or quantum) if we can get information about one spin by looking at the other. Let us analyze three

following scenarios, supposing that we want to learn about the second spin by looking at the first one.

(i) If the two-spin density operator is $|00\rangle\langle 00|$, for any local measurement applied to the first spin, the second one is in the state $|0\rangle$, so there is no correlation at all between the two spins.

(ii) Consider now the two-spin density operator $(1/2)(|00\rangle\langle 00| + |11\rangle\langle 11|)$. If we selectively measure the first spin by adjusting the apparatus in the computational basis, we can predict the value of the second spin with certainty, although we cannot predict the value of the second spin with certainty before measuring the first spin. In this case, the state is fully classically correlated.

(iii) In the last example, the two-spin density operator is $(1/2)(|00\rangle\langle 00| + |-1\rangle\langle -1|)$, with $|-\rangle = (1/\sqrt{2})(|0\rangle - |1\rangle)$. For this state, there is no local measurement over the first spin that reveals the value of the second spin with certainty on average. If we measure the first spin in the state $|0\rangle$, the second spin is in a statistical mixture of $|0\rangle$ and $|1\rangle$. Equivalently, there is no non-selective measurement of the form of Eq. (5) that is capable of leaving the density operator undisturbed. Thus, besides classical correlation, we also have quantum discord.

For a quantum chain with more than two spins, two-qubit states are described by the reduced density operator ρ obtained after tracing out all spins of the chain except the two selected ones. For Hamiltonians that commute with the parity operator $\otimes_{i=1}^{N} S_i^z$, as H in Eq. (1), the reduced density matrix written in the computational basis has the form

$$\rho = \begin{pmatrix} \rho_{11} & 0 & 0 & \rho_{41}^* \\ 0 & \rho_{22} & \rho_{32}^* & 0 \\ 0 & \rho_{32} & \rho_{33} & 0 \\ \rho_{41} & 0 & 0 & \rho_{44} \end{pmatrix} , \qquad (9)$$

where the following constraints are assumed: $\sum_{i=1}^{4} \rho_{ii} = 1$ (normalization condition), $\rho_{11}\rho_{44} \geq |\rho_{41}|^2$, and $\rho_{22}\rho_{33} \geq |\rho_{32}|^2$ (positive semidefiniteness). The nonzero elements ρ_{ij} appear only in the diagonal and anti-diagonal of the reduced density matrix, which justifies the label "X-state". For this kind of two-qubit states, there are analytical expressions to calculate the geometric correlations [89, 90]. Indeed, defining the following auxiliary parameters

$$c_1 = 2(\rho_{32} + \rho_{41}),\ c_2 = 2(\rho_{32} - \rho_{41}),$$

$$c_3 = 1 - 2(\rho_{22} + \rho_{33}),\ c_4 = 2(\rho_{11} + \rho_{33}) - 1,$$

$$c_5 = 2(\rho_{11} + \rho_{22}) - 1,$$

the geometric quantum discord is given by [89]

$$Q_G(\rho) = \sqrt{\frac{ac - bd}{a - b + c - d}} , \qquad (10)$$

where $a = \max(c_3^2, d + c_5^2)$, $b = \min(c, c_3^2)$, $c = \max(c_1^2, c_2^2)$ and $d = \min(c_1^2, c_2^2)$. The geometric classical and total correlations are respectively written as [90]

$$C_G(\rho) = c_{\max}, \qquad (11)$$

$$T_G(\rho) = \frac{1}{2}\left[c_{\max} + \max(c_{\max}, c_{\text{int}} + c_{\min})\right] , \qquad (12)$$

where $c_{\max} = \max(|c_1|, |c_2|, |c_3 - c_4 c_5|)$, $c_{\min} = \min(|c_1|, |c_2|, |c_3 - c_4 c_5|)$, and $c_{\text{int}} = \text{int}(|c_1|, |c_2|, |c_3 - c_4 c_5|)$ corresponds to the intermediate value.

The geometric quantum discord Q_G between two nearest-neighboring spins is shown in the main panel of Fig. 2 as a function of h/J for different chain sizes. The classical and total correlations, C_G and T_G, are displayed in Figs. 3 (a) and 3 (b). The curves for the quantum, classical, and total correlations exhibit a similar pattern. They are non-monotonic and generalize the behavior of pairwise entanglement, as measured by concurrence [11, 15]. We identify the following three regions, described below.

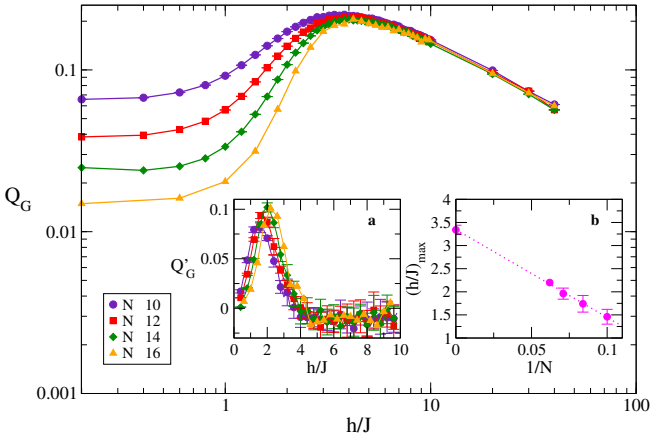

FIG. 2: (Color online) Main panel: Geometric quantum discord Q_G as function of the disorder strength h/J in a logarithmic scale. Inset (a): first derivative Q'_G of the geometric quantum discord with respect to h/J. Inset (b): the thermodynamic limit of the maximum of Q'_G, which yields $h_c/J = 3.34 \pm 0.03$.

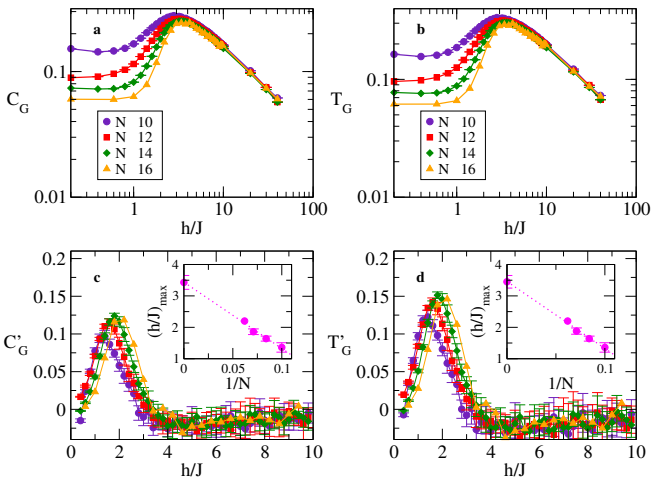

FIG. 3: (Color online) Geometric classical C_G (a) and total T_G (b) correlations as functions of h/J in logarithmic scale, as well as their derivatives, C'_G (c) and T'_G (d), with respect to h/J. The insets in (c) and (d) exhibit the thermodynamic limit of the maxima of C'_G and T'_G, respectively, yielding $h_c/J = 3.43 \pm 0.06$ for C_G and $h_c/J = 3.45 \pm 0.06$ for T_G.

In the chaotic phase, $0 < h/J < 1$, the correlations are spread out in the system in a multipartite form [12]. This results in a small concentration of correlations between individual pairs of spins and explains the small values of Q_G, C_G, and T_G.

As the disorder strength increases beyond the chaotic region, $h/J > 1$, one sees that Q_G, C_G, and T_G increase up to a value of h/J that depends on the length of the system. In the vicinity of the MBL transition, correlations are mostly confined between individual pairs of spins, which gives rise to the large values of the quantum, classical, and total pairwise correlations.

After the transition to the MBL phase, further increasing the disorder strength asymptotically decreases the correlation measures due to the reduction of the effective role played by the exchange interaction J. Like the global entanglement, the correlations Q_G, C_G and T_G show a power-law decay $\propto (h/J)^{-\beta}$ deep in the localized phase, with a universal exponent roughly given by $\beta = 0.7$. For a finite system, pairwise correlations tend to disappear in the limit of infinite disorder.

The qualitative behavior of the quantum, classical, and total correlation measures discussed above suggests the existence of a localized phase. The location of the critical point can now be achieved by analyzing the first derivative of the correlation measures with respect to the disorder strength h/J. This approach is inspired by the procedure used in studies of ordinary quantum phase transitions (at zero temperature), either via pairwise entanglement [6, 7] or via pairwise quantum discord [9, 10]. It is worth stressing that since quantum discord reveals quantumness in separable mixed states, it manifests its presence in scenarios beyond entanglement. For instance, in contrast to entanglement, quantum discord can characterize quantum phase transitions also at finite temperatures, as it actually occurs in experimental realizations [83]. Moreover, quantum discord usually survives longer than entanglement as a function of the distance between the spins. More specifically, quantum discord exhibits power-law decay along the chain in critical phases [84], whereas pairwise entanglement (as measured, e.g., by concurrence) consistently shows short-range behavior, vanishing for a few-distant sites even at the critical point [6]. These robust properties of the quantum discord should be advantageous for the characterization of the MBL transition at high temperatures and if distant spins are to be considered in real setups.

As illustrated in the inset (a) of Fig. 2 and in Figs. 3 (c) and 3 (d), the three correlation measures exhibit a maximum in their derivatives, which occurs at a value of h/J denoted by $(h/J)_{\max}$. The maxima of the derivatives of the correlation measures obey a linear decay with $1/N$, from where the critical point can be obtained by extrapolating $(h/J)_{\max}$ for $N \to \infty$.

The scaling analysis of $(h/J)_{\max}$, shown in the inset (b) of Fig. 2 and in the insets of Figs. 3 (c) and 3 (d), leads to $h_c/J \in [3, 4]$, which coincides with the range of values for the critical point found in previous works. Table I provides the values of the critical point extracted from each geometric correlation measure and also from the global entanglement G_E. The critical values obtained with the four different quantities

Correlation measure	h_c/J
G_E	3.8 ± 0.2
Q_G	3.34 ± 0.03
C_G	3.43 ± 0.06
T_G	3.45 ± 0.06

TABLE I: Critical point obtained via global entanglement in comparison with quantum, classical, and total geometric correlations. Error bars account only for fluctuations with respect to the number disorder realizations.

are compatible with each other. This confirms that the picture of delocalization of correlations in the thermal phase against concentration of correlations in the vicinity of the MBL critical point holds for quantum, classical, and total correlations between spin pairs. We notice that the error bars computed here account only for fluctuations with respect to the number disorder realizations. Other possible sources of uncertainty are not taken into account.

V. CONCLUSIONS

We have described the transition to the MBL phase and located its critical point with pairwise correlation measures that involve one or at most two-point correlation functions. The results converged by taking only a small fraction of the eigenstates of the Hamiltonian. Our main findings are:

(i) The finite size scaling analysis of the global entanglement led to the critical point $h_c/J = 3.8 \pm 0.2$, which coincides with the result from previous works. This quantity, as computed here, is the linear entropy of a single spin. It is impressive that a simple one-point correlation function can be so effective at identifying the critical point.

(ii) The geometric correlations between only two spins located the critical point in the range of $h_c/J \in [3, 4]$, which is also within acceptable values. The procedure used resembles the one adopted in the analysis of ordinary quantum phase transitions, where the critical point is revealed by the derivative of the correlation measures. The scaling analysis of the derivatives of the quantum, classical, and total correlations followed the universal linear scaling law, that is, the derivatives are linear functions of $1/N$. The critical point is obtained by the extrapolation to the thermodynamic limit.

When compared with pairwise entanglement measures, such as concurrence, quantum discord offers important advantages. Its robust properties with respect to temperature and distance between the spins turns the quantum discord into a powerful criticality witness.

As a byproduct of our analysis, we found a non-monotonic behavior of the global entanglement in the transition from the clean integrable limit to the chaotic regime. A detailed characterization of the onset of chaos in terms of pairwise correlations is left as a plan for further studies. In the future, it might also be interesting to explore the effectiveness of the one and two-point correlation functions in the detection of the metal-insulator transition in higher dimensions. Another aspect that we intend to investigate is the changes that should be brought

to the picture developed here when time-dependent Hamiltonians or the presence of decoherence are taken into account.

Acknowledgments

J.L.C.C.F. is supported by CAPES-Brazil. A.S. thanks Stephan Haas for the use of the HPC cluster and for his hospitality at the University of Southern California, where this work initiated. L.F.S. is supported by the NSF grant No. DMR-1603418. M.S.S. acknowledges support from CNPq-Brazil (No.303070/2016-1), FAPERJ (No 203036/2016), and the Brazilian National Institute for Science and Technology of Quantum Information (INCT-IQ).

[1] U. Schollwöck, Ann. of Phys. **326**, 96 (2011).
[2] G. Tóth and I. Apellaniz, J. Phys. A **47**, 424006 (2014).
[3] P. Hayden and J. Preskill, JHEP **2007**, 120 (2007).
[4] L. Amico, R. Fazio, A. Osterloh, and V. Vedral, Rev. Mod. Phys. **80**, 517 (2008).
[5] H. Li and F. D. M. Haldane, Phys. Rev. Lett. **101**, 010504 (2008).
[6] A. Osterloh, L. Amico, G. Falci, and R. Fazio, Nature **416**, 608 (2002).
[7] L.-A. Wu, M. S. Sarandy, and D. A. Lidar, Phys. Rev. Lett. **93**, 250404 (2004).
[8] V. E. Korepin, Phys. Rev. Lett. **92**, 096402 (2004).
[9] M. S. Sarandy, Phys. Rev. A **80**, 022108 (2009).
[10] R. Dillenschneider, Phys. Rev. B **78**, 224413 (2008).
[11] L. F. Santos, G. Rigolin, and C. O. Escobar, Phys. Rev. A **69**, 042304 (2004).
[12] W. G. Brown, L. F. Santos, D. Starling, and L. Viola, Phys. Rev. E **77**, 021106 (2008).
[13] F. Dukesz, M. Zilbergerts, and L. F. Santos, New J. Phys. **11**, 043026 (2009).
[14] C. Mejia-Monasterio, G. Benenti, G. Carlo, and G. Casati, Phys. Rev. A **71**, 062324 (2005).
[15] S. Bera and A. Lakshminarayan, Phys. Rev. B **93**, 134204 (2016).
[16] J. A. Kjäll, J. H. Bardarson, and F. Pollmann, Phys. Rev. Lett. **113**, 107204 (2014).
[17] Z.-C. Yang, C. Chamon, A. Hamma, and E. R. Mucciolo, Phys. Rev. Lett. **115**, 267206 (2015).
[18] J. Goold, C. Gogolin, S. R. Clark, J. Eisert, A. Scardicchio, and A. Silva, Phys. Rev. B **92**, 180202 (2015).
[19] G. De Tomasi, S. Bera, J. H. Bardarson, and F. Pollmann, Phys. Rev. Lett. **118**, 016804 (2017).
[20] J. Smith, A. Lee, P. Richerme, B. Neyenhuis, P. W. Hess, P. Hauke, M. Heyl, D. A. Huse, and C. Monroe, Nat. Phys. **12**, 907 (2016).
[21] K. X. Wei, C. Ramanathan, and P. Cappellaro, arXiv:1612.05249.
[22] P. W. Anderson, Phys. Rev. **109**, 1492 (1958).
[23] S. Aubry and G. André, Ann. Isr. Phys. Soc. **3**, 1335 (1980).
[24] Y. Avishai, J. Richert, and R. Berkovitz, Phys. Rev. B **66**, 052416 (2002).
[25] L. F. Santos, J. Phys. A **37**, 4723 (2004).
[26] R. V. Jensen and R. Shankar, Phys. Rev. Lett. **54**, 1879 (1985).
[27] V. Zelevinsky, B. A. Brown, N. Frazier, and M. Horoi, Phys. Rep. **276**, 85 (1996).
[28] F. Borgonovi, F. M. Izrailev, L. F. Santos, and V. G. Zelevinsky, Phys. Rep. **626**, 1 (2016).
[29] L. D'Alessio, Y. Kafri, A. Polkovnikov, and M. Rigol, Adv. Phys. **65**, 239 (2016).
[30] L. Fleishman and P. W. Anderson, Phys. Rev. B **21**, 2366 (1980).
[31] T. Giamarchi and H. J. Schulz, Phys. Rev. B **37**, 325 (1988).
[32] I. V. Gornyi, A. D. Mirlin, and D. G. Polyakov, Phys. Rev. Lett. **95**, 206603 (2005).
[33] D. M. Basko, I. L. Aleiner, and B. L. Altshuler, Ann. Phys. **321**, 1126 (2006).
[34] I. L. Aleiner, B. L. Altshuler, and G. V. Shlyapnikov, Nat. Phys. **6**, 900 (2010).
[35] J. Z. Imbrie, J. Stat. Phys. **163**, 998 (2016).
[36] L. F. Santos, M. I. Dykman, M. Shapiro, and F. M. Izrailev, Phys. Rev. A **71**, 012317 (2005).
[37] V. Oganesyan and D. A. Huse, Phys. Rev. B **75**, 155111 (2007).
[38] M. Žnidarič, T. Prosen, and P. Prelovšek, Phys. Rev. B **77**, 064426 (2008).
[39] A. Pal and D. A. Huse, Phys. Rev. B **82**, 174411 (2010).
[40] E. Canovi, D. Rossini, R. Fazio, G. E. Santoro, and A. Silva, Phys. Rev. B **83**, 094431 (2011).
[41] J. H. Bardarson, F. Pollmann, and J. E. Moore, Phys. Rev. Lett. **109**, 017202 (2012).
[42] A. D. Luca and A. Scardicchio, Europhys. Lett. **101**, 37003 (2013).
[43] D. A. Huse, R. Nandkishore, and V. Oganesyan, Phys. Rev. B **90**, 174202 (2014).
[44] Y. Bar Lev and D. R. Reichman, Phys. Rev. B **89**, 220201 (2014).
[45] T. Grover, arXiv:1405.1471.
[46] M. Serbyn, Z. Papić, and D. A. Abanin, Phys. Rev. B **90**, 174302 (2014).
[47] A. Chandran and C. R. Laumann, Phys. Rev. B **92**, 024301 (2015).
[48] D. J. Luitz, N. Laflorencie, and F. Alet, Phys. Rev. B **91**, 081103 (2015).
[49] D. J. Luitz, N. Laflorencie, and F. Alet, Phys. Rev. B **93**, 060201 (2016).
[50] E. J. Torres-Herrera and L. F. Santos, Phys. Rev. B **92**, 014208 (2015).
[51] E. J. Torres-Herrera, M. Távora, and L. F. Santos, Braz. J. Phys. **46**, 239 (2016).
[52] E. Altman and R. Vosk, Ann. Rev. Cond. Mat. Phys. **6**, 383 (2015).
[53] R. Nandkishore and D. Huse, Annu. Rev. Cond. Mat. Phys. **6**, 15 (2015).
[54] M. Serbyn, Z. Papić, and D. A. Abanin, Phys. Rev. X **5**, 041047 (2015).
[55] R. Singh, J. H. Bardarson, and F. Pollmann, New J. Phys. **18**, 023046 (2016).
[56] K. Agarwal, S. Gopalakrishnan, M. Knap, M. Müller, and E. Demler, Phys. Rev. Lett. **114**, 160401 (2015).
[57] C. L. Bertrand and A. M. García-García, Phys. Rev. B **94**, 144201 (2016).
[58] S. Gopalakrishnan, K. Agarwal, E. A. Demler, D. A. Huse, and M. Knap, Phys. Rev. B **93**, 134206 (2016).

[59] C. Monthus, Entropy **18**, 122 (2016).
[60] C. Gogolin and J. Eisert, Rep. Prog. Phys. **79**, 056001 (2016).
[61] O. S. Barišić, J. Kokalj, I. Balog, and P. Prelovšek, Phys. Rev. B **94**, 045126 (2016).
[62] V. Khemani, F. Pollmann, and S. L. Sondhi, Phys. Rev. Lett. **116**, 247204 (2016).
[63] T. Enss, F. Andraschko, and J. Sirker, Phys. Rev. B **95**, 045121 (2017).
[64] E. J. Torres-Herrera and L. F. Santos, Ann. Phys. (Berlin) p. 1600284 (2017).
[65] E. J. Torres-Herrera and L. F. Santos, arXiv:1702.04363.
[66] D. J. Luitz and Y. B. Lev, arXiv:1607.01012.
[67] M. Schreiber, S. S. Hodgman, P. Bordia, H. P. Lüschen, M. H. Fischer, R. Vosk, E. Altman, U. Schneider, and I. Bloch, Science **349**, 842 (2015).
[68] S. S. Kondov, W. R. McGehee, W. Xu, and B. DeMarco, Phys. Rev. Lett. **114**, 083002 (2015).
[69] F. Iemini, A. Russomanno, D. Rossini, A. Scardicchio, and R. Fazio, Phys. Rev. B **94**, 214206 (2016).
[70] S. Campbell, M. J. M. Power, and G. De Chiara, e-print arXiv:1608.08897 (2016).
[71] D. A. Meyer and N. R. Wallach, J. Math. Phys. **43**, 4273 (2002).
[72] G. Brennen, Quantum Inf. Comput. **3**, 619 (2003).
[73] F. M. Paula, T. R. de Oliveira, and M. S. Sarandy, Phys. Rev. A **87**, 064101 (2013).
[74] T. Nakano, M. Piani, and G. Adesso, Phys. Rev. A **88**, 012117 (2013).
[75] F. M. Paula, J. D. Montealegre, A. Saguia, T. R. de Oliveira, and M. S. Sarandy, EPL (Europhys. Lett.) **103**, 50008 (2013).
[76] S. P. Walborn, P. H. Souto Ribeiro, L. Davidovich, F. Mintert, and A. Buchleitner, Nature **440**, 1022 (2006).
[77] P. Jurcevic, B. P. Lanyon, Hauke, C. P., Hempel, P. Zoller, R. Blatt, and C. F. Roos, Nature **511**, 202 (2014).
[78] T. Fukuhara, S. Hild, J. Zeiher, P. Schauß, I. Bloch, M. Endres, and C. Gross, Phys. Rev. Lett. **115**, 035302 (2015).
[79] H. Ollivier and W. H. Zurek, Phys. Rev. Lett. **88**, 017901 (2001).
[80] L. Henderson and V. Vedral, J. Phys. A **34**, 6899 (2001).
[81] S. Luo, Phys. Rev. A **77**, 022301 (2008).
[82] A. Saguia, C. C. Rulli, T. R. de Oliveira, and M. S. Sarandy, Phys. Rev. A **84**, 042123 (2011).
[83] T. Werlang, C. Trippe, G. A. P. Ribeiro, and G. Rigolin, Phys. Rev. Lett. **105**, 095702 (2010).
[84] J. Maziero, L. Céleri, R. Serra, and M. Sarandy, Phys. Lett. A **376**, 1540 (2012).
[85] O. Giraud, J. Martin, and B. Georgeot, Phys. Rev. A **76**, 042333 (2007).
[86] K. Modi, A. Brodutch, H. Cable, T. Paterek, and V. Vedral, Rev. Mod. Phys. **84**, 1655 (2012).
[87] A. Brodutch and K. Modi, Quantum Inf. Comput. **12**, 0721 (2012).
[88] F. M. Paula, A. Saguia, T. R. de Oliveira, and M. S. Sarandy, EPL (Europhys. Lett.) **108**, 10003 (2014).
[89] F. Ciccarello, T. Tufarelli, and V. Giovannetti, New J. Phys. **16**, 013038 (2014).
[90] P. C. Obando, F. M. Paula, and M. S. Sarandy, Phys. Rev. A **92**, 032307 (2015).